Cytokine 164 (2023) 156107

Contents lists available at ScienceDirect

Cytokine

journal homepage: www.elsevier.com/locate/cytokine

SPP1 exacerbates ARDS via elevating Th17/Treg and M1/M2 ratios through suppression of ubiquitination-dependent HIF-1α degradation

Liang Chen *, Jin Yang, Meng Zhang, Donglin Fu, Huan Luo, Xiaolei Yang

Intensive Care Unit, Chongqing General Hospital, Chongqing 401147, PR China

ARTICLE INFO

Keywords:
ARDS
SPP1
HIF-1α
Th17
Treg
Macrophage
Degradation

ABSTRACT

Background: Acute respiratory distress syndrome (ARDS) is a severe inflammatory pulmonary condition that leads to respiratory failure. The imbalance of Th17/Treg and M1/M2 is implicated in ARDS. A better understanding of the regulation of the balance of Th17/Treg and M1/M2 may provide novel therapeutic targets for ARDS.

Methods: Plasma and BALF samples were collected from ARDS patients. Inflammatory cytokines were examined by ELISA. Th17, Treg, M1 and M2 were identified via immunofluorescence staining of RORγt, Foxp3, iNOS and Arg-1. H&E and Masson's trichrome staining were applied for evaluating pulmonary damage and fibrosis. A mouse model of ARDS was established through LPS administration. HIF-1α was immunoprecipitated and subjected to ubiquitination analysis via western blotting. The expression of SPP1, VHL and HIF-1α was examined by RT-qPCR and western blotting.

Results: ARDS patients showed elevated levels of inflammatory cytokines and ratios of Th17/Treg and M1/M2. SPP1 was upregulated in ARDS mice, and silencing of SPP1 alleviated lung injury and fibrosis. SPP1 inhibited VHL expression to reduce the ubiquitination and degradation of HIF-1α in ARDS. Overexpression of SPP1 facilitated Th17, Treg and M1 polarization but inhibited M2 polarization through upregulation of HIF-1α.

Conclusion: SPP1 elevates Th17/Treg and M1/M2 ratio by suppressing VHL expression and ubiquitination-dependent HIF-1α degradation, thus exacerbating ARDS. Our study provides novel mechanistic insights into ARDS pathogenesis and promising therapeutic targets.

1. Introduction

As one of the most severe lung conditions, acute respiratory distress syndrome (ARDS) is characterized by pulmonary edema, widespread inflammation and severe hypoxaemia, commonly causing acute respiratory failure and even death in critically ill patients [1]. ARDS is still incurable, and the focus of treatment, such as ventilator support and extracorporeal membrane oxygenation, is supplying oxygen and supporting patients until the lungs heal [2]. The pathogenesis of ARDS is complicated, involving lung and systemic inflammation and impaired fluid management and endothelial and epithelial barriers in the lungs [3]. ARDS is driven by intense inflammatory responses, and the imbalance between anti- and pro-inflammatory cytokines in the lungs is key for the onset and development of ARDS [4,5]. Manipulating inflammatory responses is being investigated as a potential therapy for ARDS despite several attempts have failed [6]. A better understanding of the regulatory mechanisms underlying inflammatory responses in the lungs of ARDS patients contributes to developing novel targeted therapies.

T helper 17 cells (Th17) and regulatory T cells (Treg) are key regulators in maintaining inflammatory responses. Th17 promotes inflammation via producing various proinflammatory cytokines such as IL-17, IL-23 and IL-22, whereas Treg exerts anti-inflammatory functions through secretion of TGF-β and IL-10 and suppression of immune cell function [7]. Imbalance of Th17/Treg is implicated in autoimmune and inflammatory disorders including ARDS. Increased Th17/Treg ratio has been identified as a risk indicator for early ARDS, and a significant proinflammatory Th17 shift was observed in patients [8]. Moreover, mesenchymal stem cells overexpressing TGFβ1 suppressed inflammatory responses and alleviated lung injury by reducing Th17/Treg ratio in LPS-induced ARDS mice [9]. Besides, macrophages are abundant in the lungs and play key roles in regulating inflammation. Macrophages are polarized into proinflammatory M1 macrophages and anti-inflammatory M2 macrophages, and the balance of M1/M2 is an key orchestrator in ARDS at various stages [10]. LPS-induced ARDS mice

* Corresponding author at: Intensive Care Unit, Chongqing General Hospital, No.118, Xingguang Avenue, Liangjiang New Area, Chongqing 401147, PR China.
E-mail address: 1422144585@qq.com (L. Chen).

https://doi.org/10.1016/j.cyto.2022.156107
Received 14 July 2022; Received in revised form 24 November 2022; Accepted 5 December 2022
Available online 9 February 2023

showed significantly increased M1 but decreased M2 in the lungs [11]. M1 polarization is essential for initiating inflammation in ARDS, and manipulating the balance of M1/M2 favoring a M2 shift could attenuate inflammation and lung injury [11–13]. Exploring the mechanisms underlying the balance of Th17/Treg and M1/M2 is crucial for a better understanding of inflammation and pathogenesis of ARDS.

Hypoxia inducible factor 1α (HIF-1α) is an important regulator that modulates cellular responses to hypoxia and inflammation, serving key roles in maintaining oxygen homeostasis and regulating cell survival [14]. HIF-1α facilitates Th17 differentiation via activating RORγt transcription and suppresses Treg differentiation by inducing Foxp3 degradation, controlling the balance of Th17/Treg [15]. In addition, HIF-1α promotes M1 polarization through various mechanisms [16,17]. Xu et al. reported that HIF-1α was highly expressed in LPS-induced acute lung injury (ALI) mice [18]. These studies suggest that HIF-1α may be implicated in increased Th17/Treg ratio and M1 polarization in ARDS.

In this study, we investigated the regulatory mechanisms underlying abnormal HIF-1α expression in ARDS and explored its roles in regulating Th17, Treg, M1 and M2 polarization. We demonstrated that secreted phosphoprotein 1 (SPP1) exacerbated pulmonary inflammation in ARDS via modulating the balance of Th17/Treg and M1/M2 through HIF-1α. Our study provides novel mechanistic insights into the pathogenesis of ARDS and potential therapeutic targets for ARDS.

2. Methods

2.1. Clinical specimens

Patients who were diagnosed with ARDS at Chongqing General Hospital were divided into three groups based on degrees of severity: mild (200 mmHg < PaO2/FiO2 (P/F) ≤ 300 mmHg, n = 17) moderate (100 mmHg < P/F ≤ 200 mmHg, n = 31) and severe (P/F ≤ 100 mmHg, n = 19) groups [19]. Blood and bronchoalveolar lavage fluid (BALF) samples were collected from patients and healthy donors (n = 17). Blood in anticoagulant-treated tubes was centrifugated at 2000 g for 15 min for plasma preparation.

2.2. Animals and reagents

C57BL/6 mice (male, six-week-old) were purchased from SJA Laboratory Animal Co., ltd (Changsha, Hunan, China) and kept in a specific pathogen free facility. Primary antibodies against human Foxp3 (MA5-14662), human iNOS (MA5-17139), human RORγt (PA5-86733), human/mouse SPP1 (PA5-34579) and Alexa Fluor 488 or Alexa Fluor 555-conjugated secondary antibodies (A-11008 and A-21422) were purchase from Thermo Fisher Scientific (Waltham, MA, USA). Primary antibodies against human VHL (ab270968), human HIF-1α (ab179483), human/mouse GAPDH (ab8245) and ubiquitin (ab19247) were obtained from Abcam (Cambridge, UK). DAPI (C1002), MG-132 (S1748), Trizol (R0016), SYBR Green qPCR Mix (D7260) and Hematoxylin and Eosin (H&E) Staining Kit (C0105) were provided by Beyotime (Shanghai, China). High-Capacity cDNA Reverse Transcription Kit and Neon™ Transfection System were purchased from Thermo Fisher Scientific. SiRNAs against VHL (si-VHL), SPP1 (si-SPP1) and HIF-1α (si-HIF-1α), scrambled sequences (si-NC) and lentiviral shRNA-SPP1 vectors were synthesized by GenePharma (Shanghai, China). Human $CD4^+$ T Cell Isolation Kit and Monocyte Isolation Kit were provided by STEMCELL (Vancouver, Canada). ELISA kits for IL-6, IL-17, IL-10, TGF-β, TNF-α, IL-1β, IL-4 and IL-13 were bought from Abcam.

2.3. A mouse model of ARDS

Mice were blindly divided into four groups (n = 8 per group): control, ARDS, LV-sh-NC and LV-sh-SPP1. ARDS mice were intratracheally administrated with LPS (2 mg/kg). In LV-sh-NC and LV-sh-SPP1 groups, mice received lentiviral sh-NC and sh-SPP1 particles followed by LPS administration. Control mice received an equivalent volume of normal saline. After 3 days, blood and BALF samples were collected. Subsequently, mice were sacrificed, and lung tissues were excised for histological staining.

2.4. Isolation of $CD4^+$ T cells and monocytes

Whole blood was collected from ARDS patients, and mononuclear cells were preliminarily separated through Percoll gradients. Subsequently, $CD4^+$ T cells and monocytes were isolated using Human $CD4^+$ T Cell Isolation Kit and Human Monocyte Isolation Kit according to the manufacturer's recommendations. The purity of isolated cells was > 90 %.

2.5. Reverse transcription real-time quantitative PCR (RT-qPCR)

Partial lung tissues from mice were snap-frozen and homogenized in liquid nitrogen. Lung homogenates, $CD4^+$ T cells and monocyte-macrophages were resuspended in Trizol reagent, and total RNA was extracted. Subsequently, RNA was reversely transcribed into cDNA with High-Capacity cDNA Reverse Transcription Kit. Real-time quantitative PCR was applied to analyze the relative gene expression of SPP1, RORγt, Foxp3, iNOS, Arg-1, VHL and HIF-1α. GAPDH was used as a normalization control. The $2^{-\triangle\triangle Ct}$ formula was used for calculation. Primers were shown in **Table 1**.

2.6. Western blotting

Lung homogenates, $CD4^+$ T cells and monocyte-macrophages were lysed in RIPA lysis buffer on ice for 30 mins, and total lysates were collected followed by protein quantification. Protein (30 μg) was electrophoresed and transferred to polyvinylidene fluoride membranes. Membranes were incubated with anti-SPP1 (1:500), anti-VHL (1:1000) and anti-HIF-1α (1:1000) overnight. Subsequently, membranes were washed and incubated with an HRP-conjugated secondary antibody (1:5000) for 1 h. Bands were visualized using ECL substrate, and intensity was analyzed using the ImageJ software.

2.7. Ubiquitination analysis of HIF-1α

Cells were lysed, and supernatants were collected. An anti-HIF-1α antibody (2 μg) was mixed with the supernatants and incubated for 12 h. Normal IgG isotype was used a negative control. The following day, HIF-1α was immunoprecipitated using protein A/G magnetic beads and eluted. Subsequently, the immunoprecipitated fraction was electrophoresed and transferred to polyvinylidene fluoride membranes. The ubiquitination of HIF-1α was examined with a ubiquitin antibody (1:1000). Membranes were incubated with an HRP-conjugated secondary antibody (1:5000), and bands were visualized using ECL substrate.

2.8. Enzyme-linked immunosorbent assay (ELISA)

Blood and BALF were collected from ARDS patients at Chongqing General Hospital. Blood in anticoagulant-treated tubes was centrifugated at 2000 g for 15 min for plasma preparation. BALF was collected from mice as previously described [20]. Plasma and BALF were stored at −80 °C until use. The concentrations of IL-6, IL-17, IL-10, TGF-β, TNF-α, IL-1β, IL-4 and IL-13 were examined using ELISA kits following manuals.

2.9. Immunofluorescence (IF) staining

Cells were washed, fixed in 4 % formaldehyde solution for 10 mins and permeabilized in 0.1 % Triton-X100 solution for 15 mins. Cells were blocked in 5 % goat normal serum and incubated with anti-Foxp3 (1:200), anti-RORγt (1:200), anti-iNOS (1:500) and anti-Arg-1

(1:1000) overnight. After wash, cells were incubated with Alexa Fluor 488 and Alexa Fluor 555-conjugated secondary antibodies. DAPI was used to stain the nuclei. Cells were mounted and imaged.

2.10. Histological staining

The lungs were excised from mice and fixed in 4 % formaldehyde solution. Subsequently, the lungs were dehydrated, embedded in paraffin and sliced into 5-μm sections. Sections were deparaffinized in xylene and rehydrated. Hematoxylin and eosin staining was applied to evaluate lung damage. For Masson's trichrome staining, sections were mordanted and stained in Weigert's iron hematoxylin solution. Sections were mounted and imaged with an Olympus BX51 microscope.

2.11. Statistical analysis

Data from at least three independent assays were analyzed by the Student's test or one-way analysis of variance (ANOVA) with the Tukey's post hoc test and expressed as mean ± standard deviation (SD). $P < 0.05$ was statistically significant. $^{*}P < 0.05$, $^{**}P < 0.01$ and $^{***}P < 0.001$.

3. Results

3.1. Elevated Th17/Treg and M1/M2 ratios in ARDS patients

A strong inflammatory response and subsequent cytokine storm may

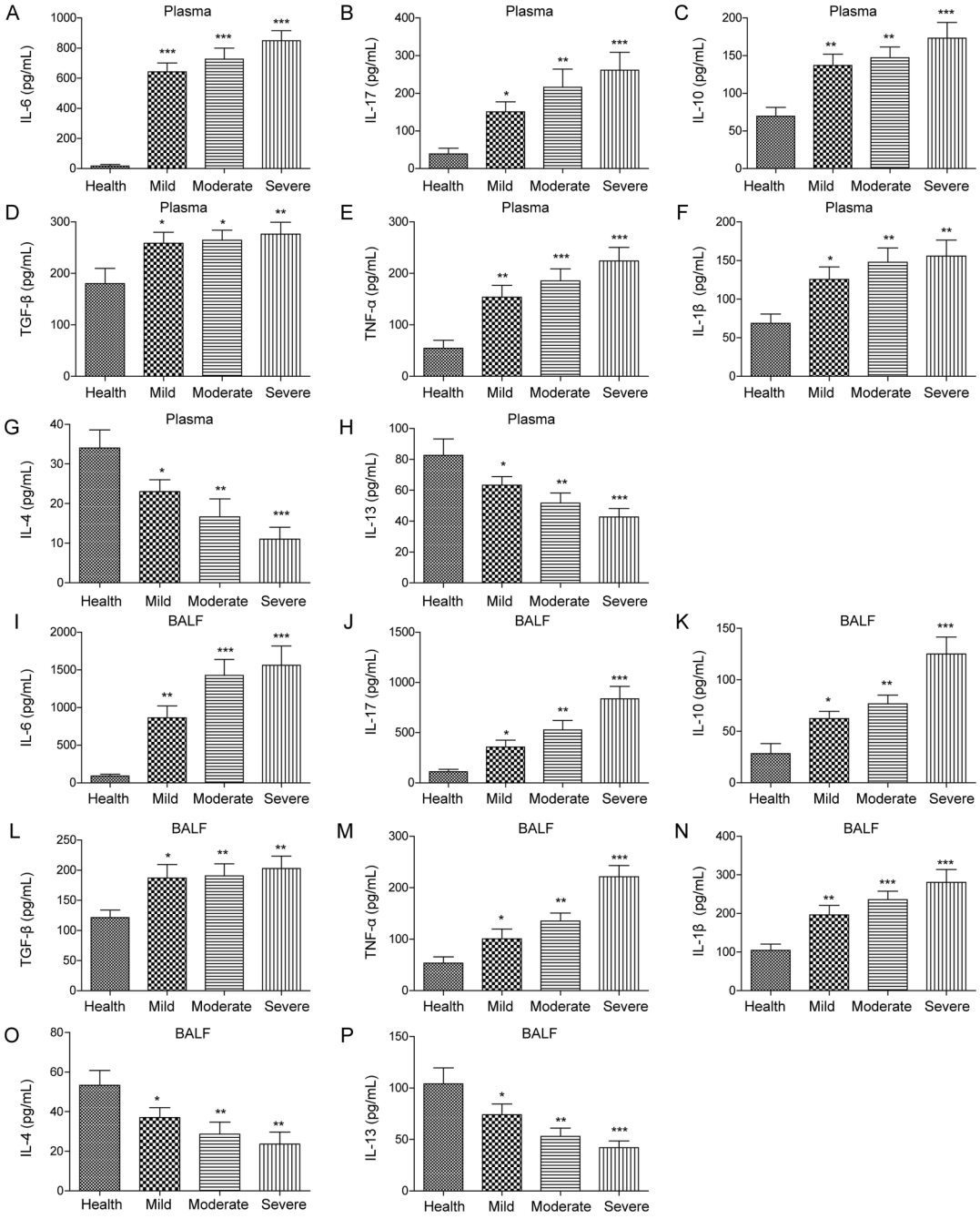

Fig. 1. Inflammatory cytokines in the plasma and BALF samples from ARDS patients. The concentration of IL-6 (A and I), IL-17 (B and J), IL-10 (C and K), TGF-β (D and L), TNF-α (E and M), IL-1β (F and N), IL-4 (G and O) and IL-13 (H and P) in plasma and BALF from healthy donors (n = 17) and ARDS patients (mild patients, n = 17; moderate patients, n = 31; severe patients, n = 19). $^{*}P < 0.05$, $^{**}P < 0.01$, and $^{***}P < 0.001$ vs Health group.

lead to ARDS [21]. Thus, we collected blood and BALF samples from ARDS patients with three degrees of severity (mild, moderate and severe) and healthy donors and examined pro- and anti-inflammatory cytokines including IL-1β, IL-4, IL-6, IL-10, IL-13, IL-17, TNF-α and TGF-β. We found elevated levels of IL-6 (Fig. 1**A and I**), IL-17 (Fig. 1**B and J**), IL-10 (Fig. 1**C and K**), TGF-β (Fig. 1**D and L**), TNF-α (Fig. 1**E and M**) and IL-1β (Fig. 1**F and N**) but reduced levels of IL-4 (Fig. 1**G and O**) and IL-13 (Fig. 1**H and P**) in plasma and BALF from patients, suggesting obvious inflammation in ARDS patients. Most of the greatest changes in these cytokines, except TGF-β, were observed in patients with severe ARDS (Fig. 1**A-P**), showing that inflammation progressively developed with increasing ARDS severity. As the balance of Th17/Treg and M1/M2 phenotype governs inflammatory responses in ARDS [9,22], we examined the abundance of Th17, Treg, M1 and M2 cells in blood samples. Compared to healthy donors, ARDS patients showed increased abundance of Treg (Foxp3 positive), Th17 (RORγt positive) and M1 (iNOS positive) cells but decreased M2 (Arg-1 positive) cells with increasing severity, and ratios of Th17/Treg and M1/M2 were greatly elevated in patients (Fig. 2**A and B**). In addition, CD86 was significantly upregulated but CD206 was downregulated in blood monocytes from ARDS patients (**Supplementary** Fig. 1). Our data indicated the imbalance of Th17/Treg and M1/M2 might control inflammation and deteriorate ARDS.

3.2. Silencing of SPP1 alleviated lung injury in ARDS mice

We analyzed gene expression in the microarray data (GSE180750) from lung tissues of bleomycin-induced pulmonary fibrosis mice to explore potential regulators of ARDS. Despite a large number of genes were differently expressed, secreted phosphoprotein 1 (SPP1), also known as osteopontin (OPN), was highly upregulated in lung tissues from bleomycin-induced mice (Fig. 3**A and B**). To investigate the role of SPP1 in ARDS, we established a mouse model of ARDS through LPS administration. Compared to control mice, ARDS mice showed high SPP1 expression in lung tissues (Fig. 3**C and D**). SPP1 was efficiently silenced in mice through lentivirus-mediated transfection of sh-SPP1 (Fig. 3**C and D**). Severe pulmonary damage and fibrosis were observed in ARDS mice (Fig. 3**E and F**). Importantly, silencing of SPP1 greatly suppressed LPS-induced pulmonary damage and fibrosis in ARDS mice (Fig. 3**E and F**). Collectively, these observations demonstrated that silencing of SPP1 alleviated lung injury in ARDS mice.

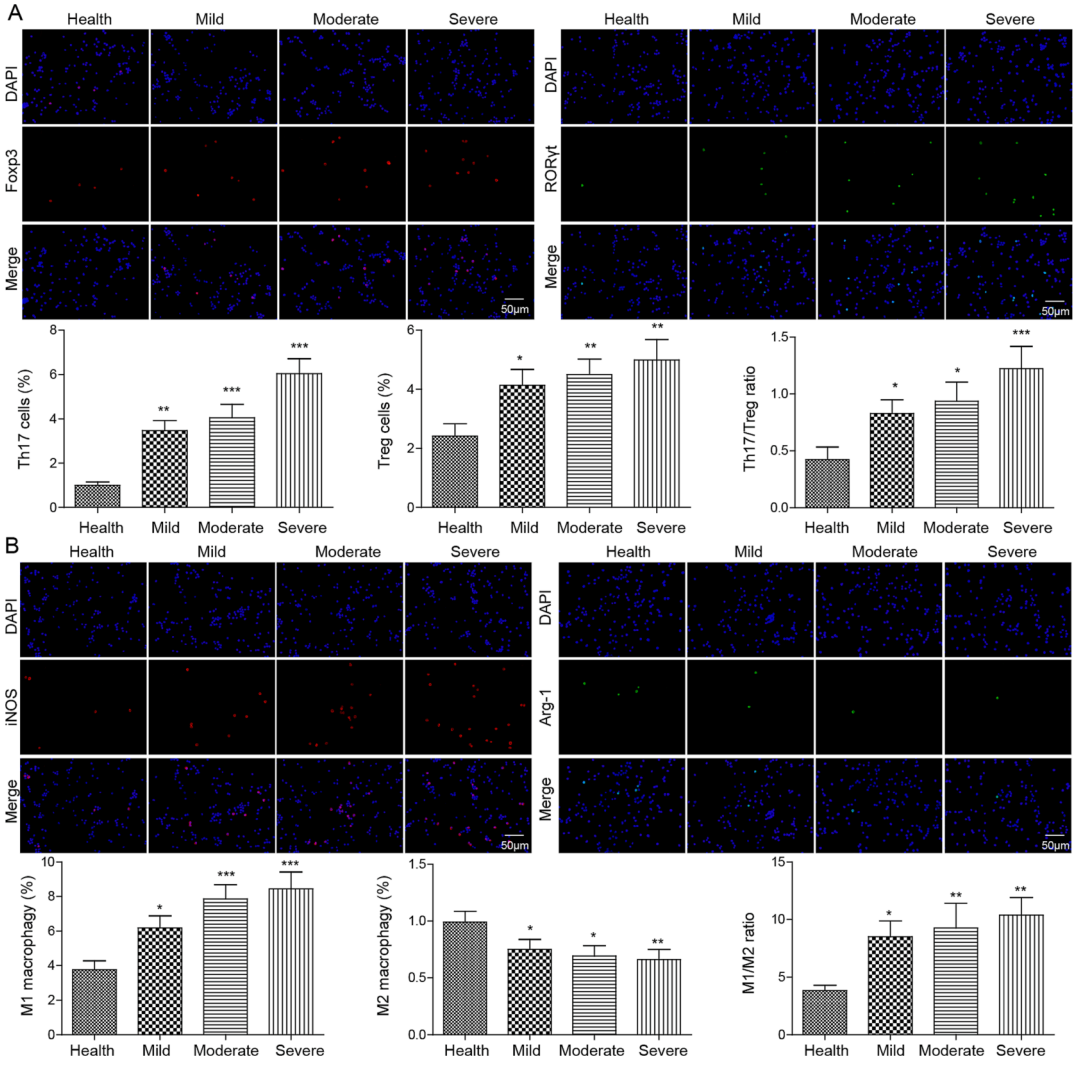

Fig. 2. Elevated Th17/Treg and M1/M2 ratios in ARDS patients. IF staining of Foxp3 (A, red), RORγt (A, green), iNOS (B, red), Arg-1 (B, green) in CD4 T cells and monocytes from healthy donors and ARDS patients. Treg (Foxp3 positive), Th17 (RORγt positive), M1 (iNOS) and M2 (Arg-1) cells were quantified, and ratios of Th17/Treg and M1/M2 were calculated. The nuclei (blue) were stained with DAPI. Scale bar, 50 μm. $^{*}P < 0.05$, $^{**}P < 0.01$, and $^{***}P < 0.001$ vs Health group. (For interpretation of the references to colour in this figure legend, the reader is referred to the web version of this article.)

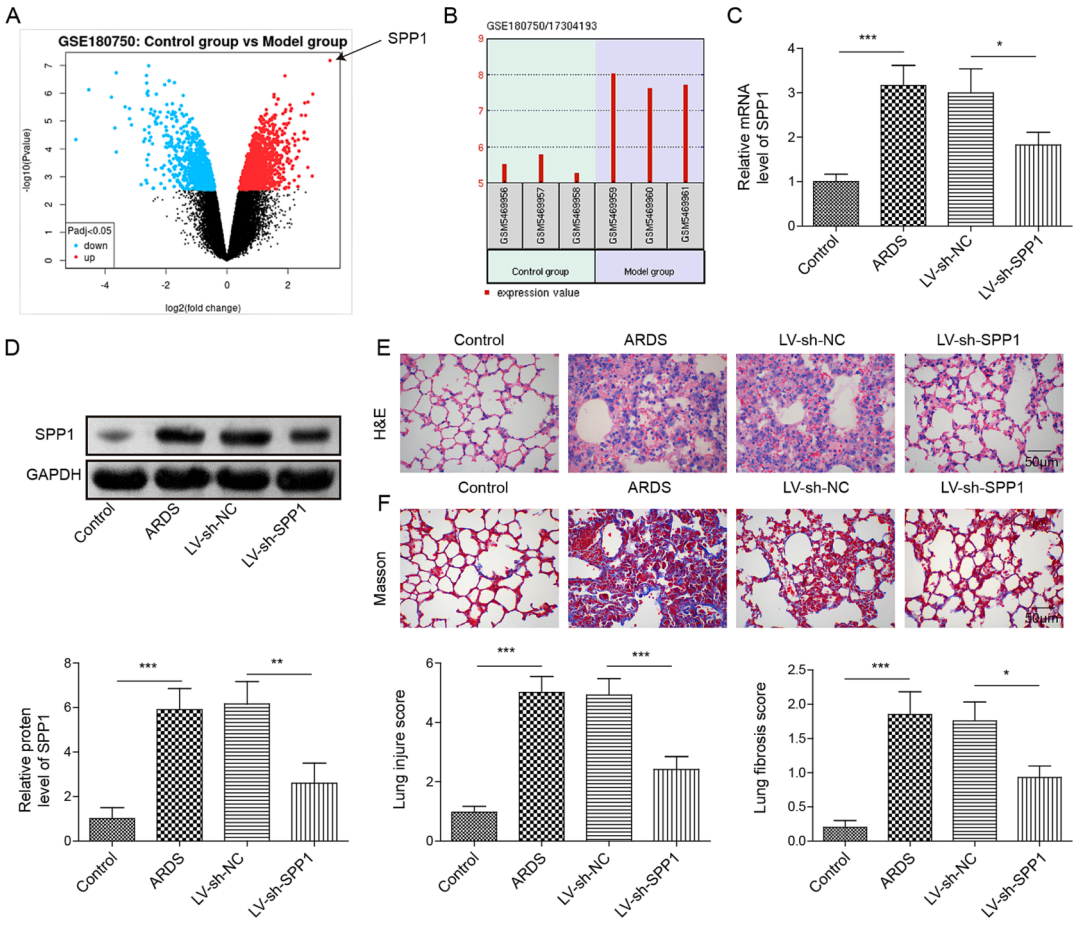

Fig. 3. Silencing of SPP1 alleviated lung injury in ARDS mice. (A) Analysis of differently expressed genes in a microarray data GSE180750. (B) High expression of SPP1 in bleomycin-induced mice from GSE180750. (C and D) RT-qPCR and western blot analysis of SPP1 in lung tissues from mice in control, ARDS, LV-sh-NC and LV-sh-SPP1 groups. (E) H&E staining of lung sections for evaluating lung damage. (F) Masson's trichrome staining for evaluating pulmonary fibrosis.

3.3. Silencing of SPP1 reduced Th17/Treg and M1/M2 ratios in ARDS mice

We further analyzed the expression of RORγt, Foxp3, iNOS and Arg-1 in ARDS mice to investigate whether SPP1 regulates the balance of Th17/Treg and M1/M2. The expression of RORγt, Foxp3 and iNOS was elevated and Arg-1 was downregulated in lung tissues from ARDS mice, whereas silencing of SPP1 reversed their expression (Fig. 4**A-D**). Moreover, increased levels of IL-6 (Fig. 4**E**), IL-17 (Fig. 4**F**), IL-10 (Fig. 4**G**), TGF-β (Fig. 4**H**), TNF-α (Fig. 4**I**) and IL-1β (Fig. 4**J**) in BALF samples from ARDS mice were largely reduced by silencing of SPP1. Elevated IL-4 and IL-13 in ARDS mice were further enhanced by knockdown of SPP1 (Fig. 4**K and L**). These results implied that silencing of SPP1 reduced Th17/Treg and M1/M2 ratios, thus alleviating pulmonary inflammation in ARDS.

4. SPP1 inhibited the ubiquitylation and degradation of HIF-1α by downregulating VHL

As SPP1 positively regulates STAT3 activation and STAT3 inhibits HIF-1α degradation through von Hippel-Lindau tumor suppressor (VHL) [23–25], we hypothesized that SPP1 might restrain VHL-mediated HIF-1α ubiquitylation and degradation in ARDS. We found that VHL was downregulated in ARDS mice but silencing of SPP1 largely restored its expression (Fig. 5**A and C**). HIF-1α was markedly upregulated in ARDS mice, and silencing of SPP1 reduced HIF-1α protein but did not affect its mRNA level (Fig. 5**B and C**), suggesting the possibility that SPP1 might regulate HIF-1α degradation. We isolated blood $CD4^+$ T cells from ARDS patients, and VHL was efficiently overexpressed or knocked down in $CD4^+$ T cells (Fig. 5**D and F**). Neither overexpression nor silencing of VHL affected the mRNA level of HIF-1α (Fig. 5**E**). However, HIF-1α protein was enhanced by knockdown of VHL but reduced by overexpression of VHL (Fig. 5**F**). SPP1 was also overexpressed or knocked down in blood $CD4^+$ T cells to identify SPP1-mediated regulation of VHL and HIF-1α (Fig. 5**G and J**). No change in HIF-1α mRNA level was observed in $CD4^+$ T cells (Fig. 5**H**). Overexpression of SPP1 reduced VHL expression and promoted HIF-1α protein, whereas knockdown of SPP1 enhanced VHL expression and reduced HIF-1α protein abundance (Fig. 5**I and J**). Subsequently, we found that overexpression of SPP1 significantly promoted HIF-1α expression and reduced its ubiquitylation, which was abrogated by simultaneous overexpression of VHL (Fig. 5**K**). In addition, knockdown of SPP1 enhanced HIF-1α ubiquitylation and reduced its protein level, and these effects were reversed by MG132 treatment (Fig. 5**L**). To be concluded, these observations suggested that SPP1 reduced HIF-1α degradation and promoted its expression via suppressing VHL expression in ARDS.

4.1. SPP1 regulated Th17, Treg, M1 and M2 polarization through HIF-1α

To explore whether SPP1 regulates the differentiation of Th17, Treg, M1 and M2 through HIF-1α in ARDS, blood $CD4^+$ T cells and monocytes were isolated from ARDS patients. Overexpression of SPP1 promoted the expression of Foxp3 and RORγt in $CD4^+$ T cells and elevated Treg and Th17 cells, but simultaneous silencing of HIF-1α reversed these effects (Fig. 6**A-D**). In addition, overexpression of SPP1 boosted iNOS expression and iNOS-positive M1 cells and reduced Arg-1 expression and Arg-

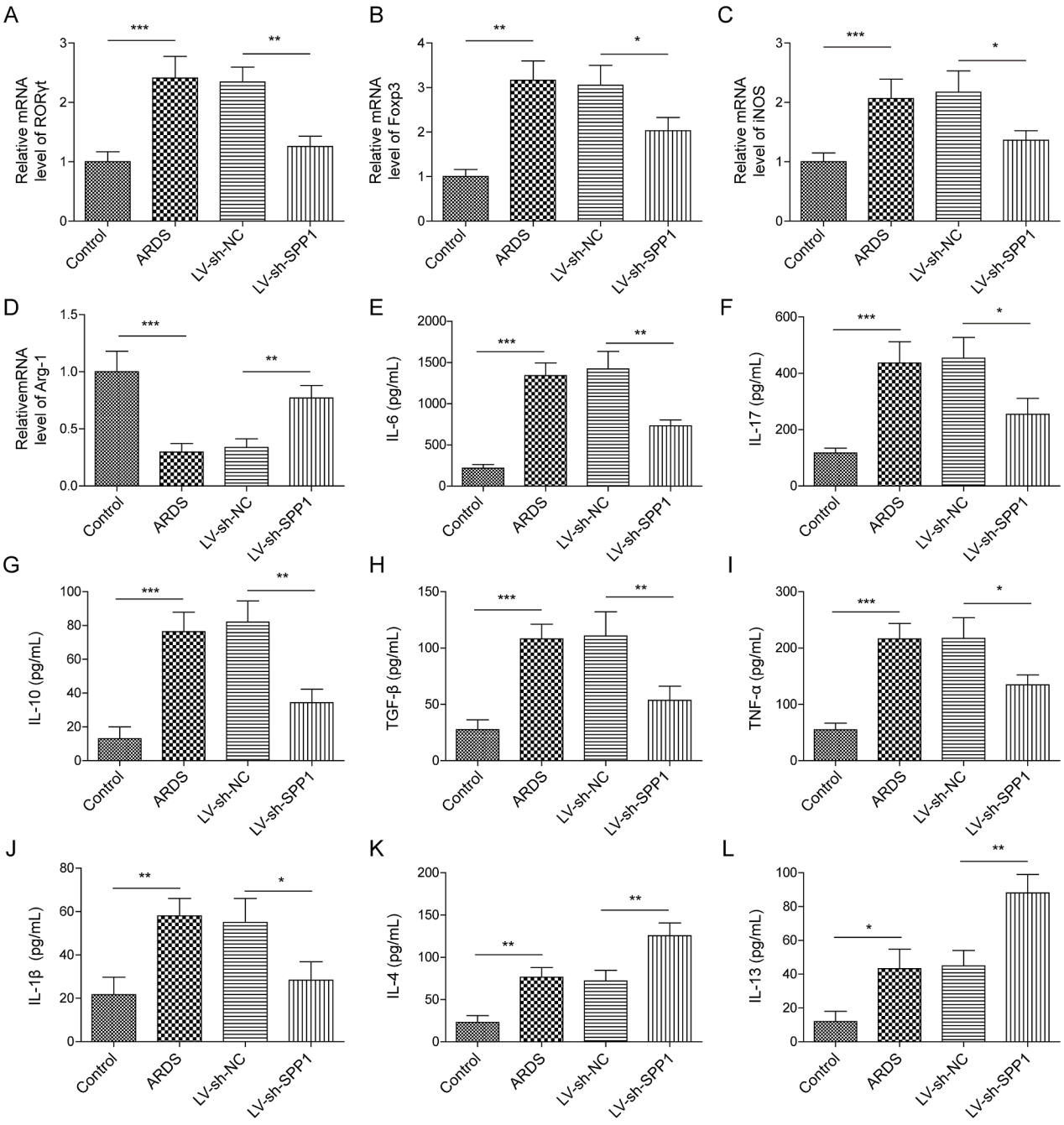

Fig. 4. Silencing of SPP1 reduced Th17/Treg and M1/M2 ratios in ARDS mice. RT-qPCR analysis of RORγt (A), Foxp3 (B), iNOS (C) and Arg-1 (D) in lung tissues from mice in control, ARDS, LV-sh-NC and LV-sh-SPP1 groups. The concentration of IL-6 (E), IL-17 (F), IL-10 (G), TGF-β (H), TNF-α (I), IL-1β (J), IL-4 (K) and IL-13 (L) in BALF.

1-positive M2 cells, which was reversed by knockdown of HIF-1α (Fig. 6**E-H**). To conclude, SPP1 facilitated Th17, Treg and M1 polarization but inhibited M2 polarization through HIF-1α.

5. Discussion

ARDS is a lethal inflammatory respiratory condition, causing accumulation of fluid in the lungs and severe hypoxemia. Management of inflammatory response has been proposed a therapeutic strategy for ARDS [26]. Elucidating the mechanisms underlying the balance of Th17/Treg and M1/M2 contributes to understanding pulmonary inflammation and has clinical significance. In present study, we observed the association of pulmonary inflammation and elevated ratios of Th17/Treg and M1/M2 in ARDS patients. Further investigation demonstrated that SPP1 promoted Th17, Treg and M1 polarization but inhibited M2 polarization by downregulating VHL and suppressing HIF-α degradation, thus aggravating pulmonary inflammation and injury in ARDS (Fig. 7).

Through analysis of the microarray data GSE180750, we found that SPP1 was highly expressed in the lungs from bleomycin-treated mice. SPP1, also known as osteopontin, modulates immune functions by recruiting leucocytes to inflammatory sites, regulating cytokine generation and cell activation and suppressing lymphocyte apoptosis, thereby inducing a pro-inflammatory microenvironment [27,28]. Specially, SPP1 drives Th17 differentiation by enhancing IL-17 production [29]. Moreover, Sangaletti et al. reported that SPP1-deficient mice showed

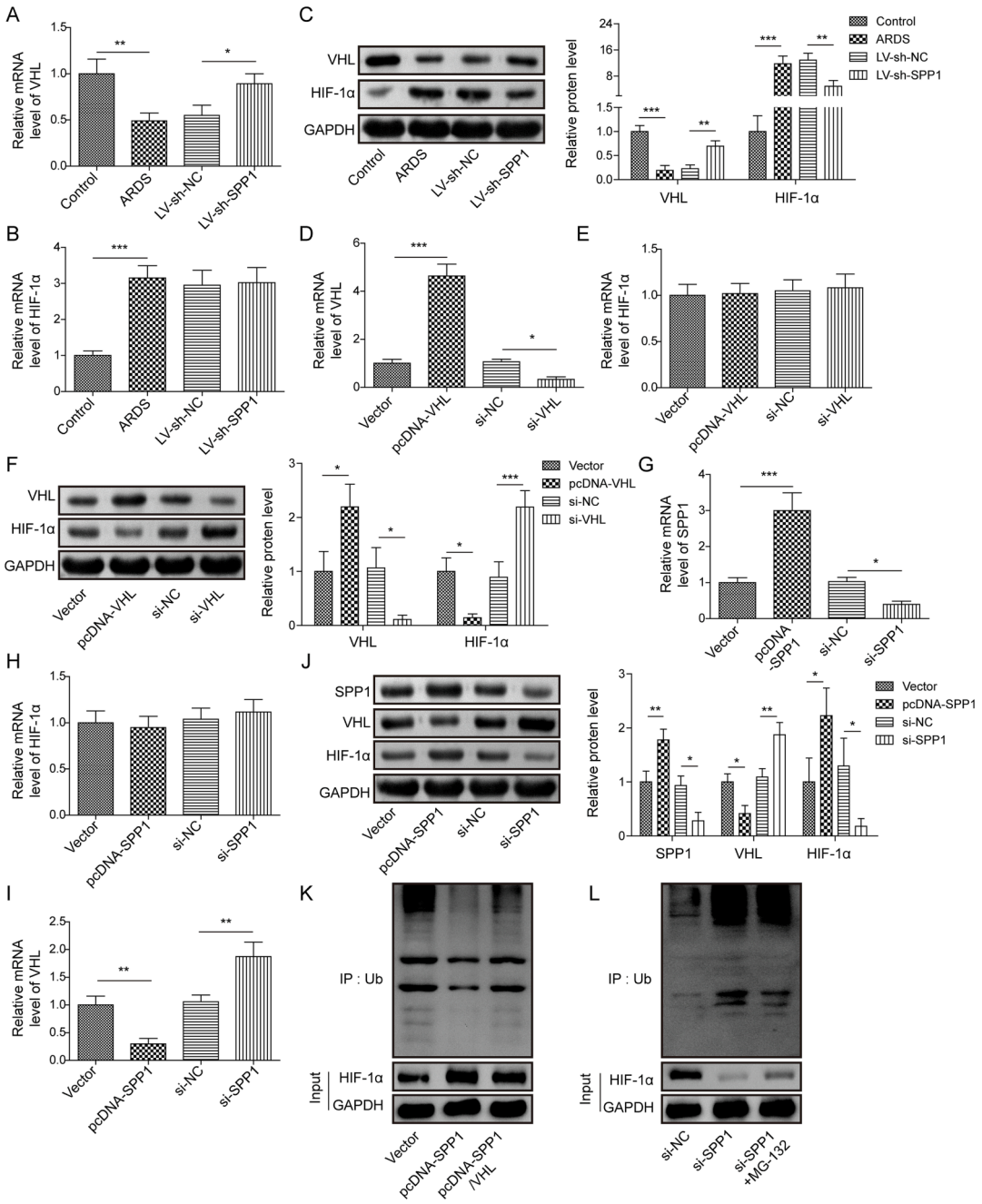

Fig. 5. SPP1 inhibited the ubiquitylation and degradation of HIF-1α by downregulating VHL. (A and B) RT-qPCR analysis of VHL and HIF-1α in lung tissues from mice in control, ARDS, LV-sh-NC and LV-sh-SPP1 groups. (C) Western blotting of VHL and HIF-1α. Blood CD4 T cells from ARDS patients were transfected with vector, pcDNA-VHL, si-NC or si-VHL. (D and E) RT-qPCR analysis of VHL and HIF-1α in CD4 T cells. (F) Western blotting of VHL and HIF-1α. CD4 T cells were transfected with vector, pcDNA-SPP1, si-NC or si-SPP1. (G, H and I) RT-qPCR analysis of SPP1, HIF-1α and VHL in CD4 T cells. (J) Western blotting of SPP1, HIF-1α and VHL. (K) Ubiquitination analysis of immunoprecipitated HIF-1α from CD4 T cells transfected with vector, pcDNA-SPP1 or pcDNA-SPP1 in combination with pcDNA-VHL. (L) Ubiquitination analysis of immunoprecipitated HIF-1α from CD4 T cells transfected with si-NC, si-SPP1 or si-SPP1 in combination with MG-132 treatment.

reduced Foxp3 + Treg cells [30], and another study found that SPP1 enhanced Treg accumulation and caused a tolerogenic environment [31]. Besides, SPP1 has been reported to be implicated in regulating macrophage polarization [32]. Fumiyuki Takahashi et al. reported increased SPP1 expression in alveolar macrophages from ARDS patients [33], and we also confirmed high expression of SPP1 in the lungs from ARDS mice. Combining with previous studies, we proposed that SPP1 might modulate inflammation by tuning the balance of Th17/Treg and M1/M2 in ARDS. Indeed, we found that silencing of SPP1 improved lung injury by reducing ratios of Th17/Treg and M1/M2 and ameliorating inflammatory responses in the lungs of ARDS mice. Besides, we observed that silencing of SPP1 reduced anti-inflammatory cytokines IL-10 and TGF-beta, which might attribute to silencing of SPP1-mediated decreased Tregs. Our findings show clinical significance of coordinating the balance of Th17/Treg and M1/M2 in management of ARDS and suggest SPP1 as a potential drug target for ARDS treatment.

Simply, macrophages were subdivided into M1 and M2. However, other macrophage subsets, such as Mhem, Mox, Mreg and M4, have been defined [34]. The roles of these non-classical macrophage subsets in ARDS are unknown. Mregs produce high levels of IL-10 and inhibit T cell

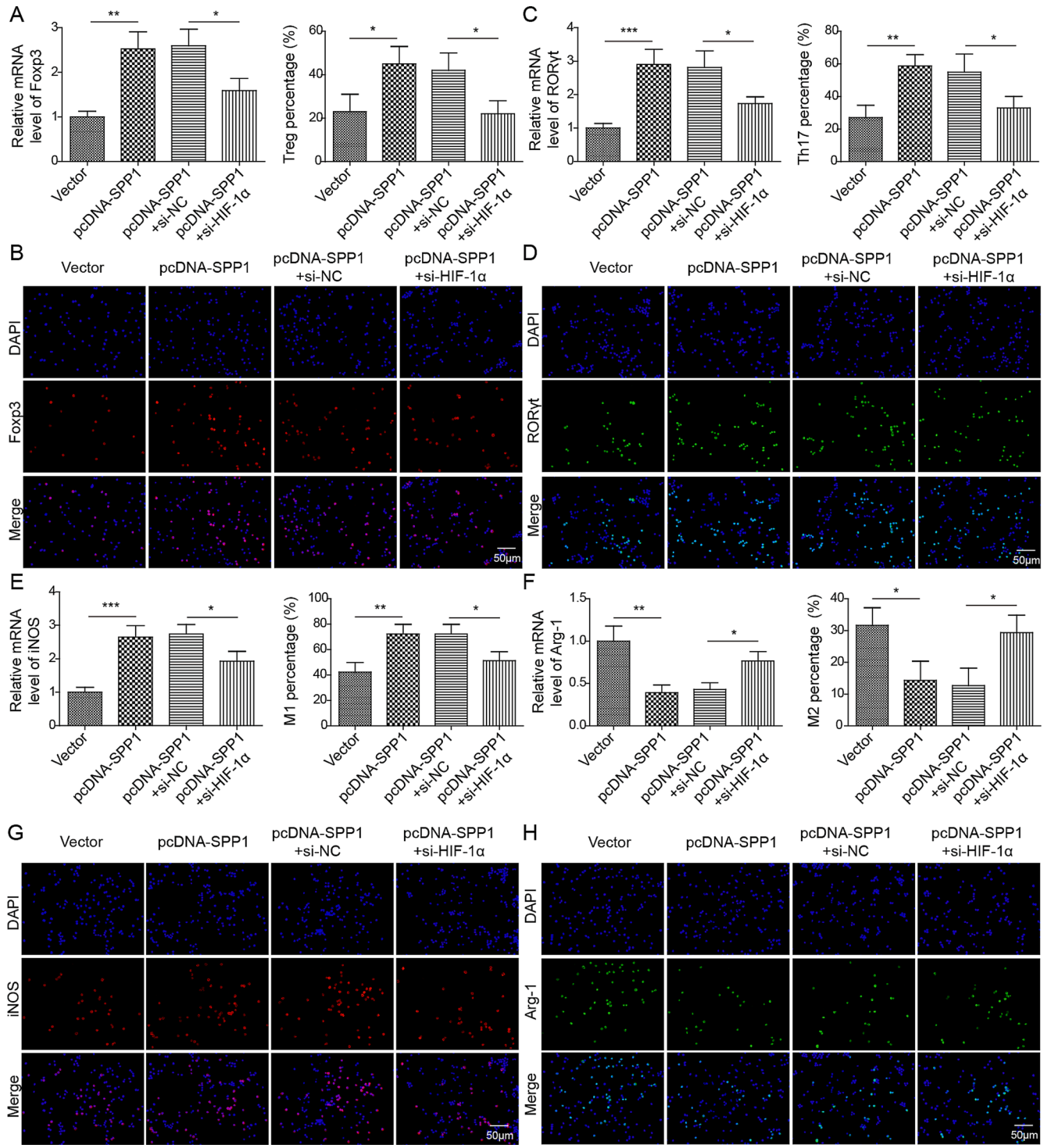

Fig. 6. SPP1 regulates Th17, Treg, M1 and M2 polarization through HIF-1α. Blood CD4 T cells from patients were transfected with vector, pcDNA-SPP1, pcDNA-SPP1 + si-NC or pcDNA-SPP1 + si-HIF-1α. (A-D) RT-qPCR analysis and IF staining of Foxp3 (red) and RORγt (green) in CD4 T cells. Blood monocytes from patients were transfected with vector, pcDNA-SPP1, pcDNA-SPP1 + si-NC or pcDNA-SPP1 + si-HIF-1α. (E-H) RT-qPCR analysis and IF staining of iNOS (red) and Arg-1 (green) in monocytes. The nuclei (blue) were stained with DAPI. Scale bar, 50 μm. (For interpretation of the references to colour in this figure legend, the reader is referred to the web version of this article.)

proliferation to regulate immune responses [35], indicating that Mregs may be implicated in pulmonary inflammation and ARDS. In addition, M2 macrophages can be further divided to M2a, M2b, M2c and M2d [36], but the specific activity of these M2 subsets in ARDS was unclear. Tu et al. reported that M2c could induce more Tregs compared to M2a although M2a and M2c did not affect the immunosuppressive function of Tregs [37]. Therefore, it would be important to figure out the activity of different macrophage subsets in various conditions.

HIF-1α is associated with increased expression of pro-inflammation cytokines favoring polarization of Th17 and M1, thus promoting subsequent inflammation [38]. It has been reported that HIF-1α promotes Th17 differentiation by directly inducing RORγt transcription but suppresses Treg differentiation through Foxp3 protein degradation [15]. However, several studies reported that HIF-1α might drive Treg

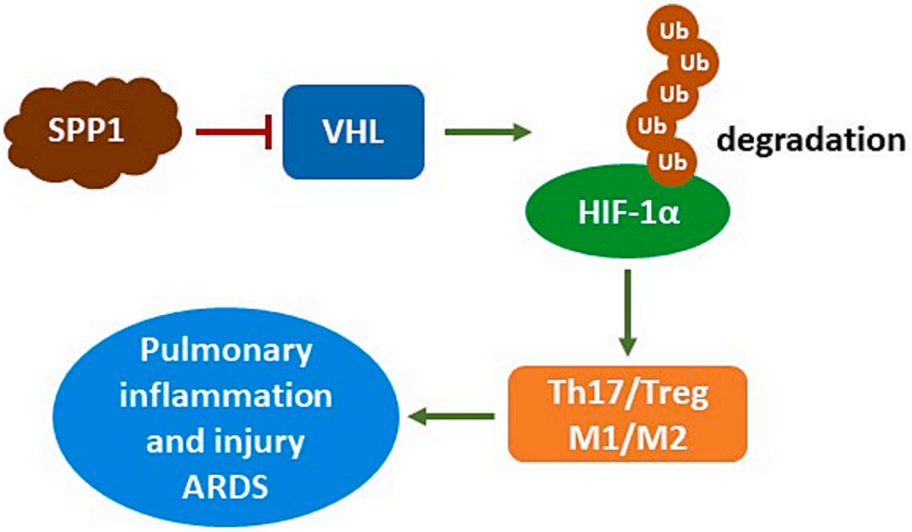

Fig. 7. The schematic diagram of this study. SPP1 inhibits VHL expression to reduce the ubiquitylation and degradation of HIF-1α, thus exacerbating ARDS.

differentiation by inducing Foxp3 expression under various conditions [39,40]. Here, we observed that silencing of HIF-1α downregulated both RORγt and Foxp3 in ARDS. The opposing activity of HIF-1α in regulating Foxp3 expression and Treg differentiation may attribute to various microenvironment conditions, which needs further investigation. In addition, suppression of HIF-1α ameliorated trauma-induced pulmonary damage [41], and HIF-1α-deficient mice showed ameliorative lung injury following lung contusion [42]. Intriguingly, we found high expression of HIF-1α in the lungs of ARDS mice, and SPP1 disrupted the balance of Th17/Treg and M1/M2 through HIF-1α, thus exacerbating ARDS. Our data suggests HIF-1α is an attractive drug target for ARDS treatment. However, a previous study reported an unexpected protective role of HIF-1α in ALI, where HIF-1α improved lung injury via controlling carbohydrate metabolism and dampening inflammation [43]. The opposing activity of HIF-1α in lung injury, promotion or protection, may resulted from various inflammatory stages and microenvironment and upstream and downstream signaling pathways. Further investigation of mechanisms underlying dual roles of HIF-1α in lung injury has important clinical significance.

Ubiquitylation-dependent protein degradation is a key mechanism to govern protein quality and abundance [44]. HIF-1α is degraded in a ubiquitination-dependent manner through various mechanisms. For instance, Koh and colleagues found that the E3-ubiquitin ligase HAF promoted the proteasome-dependent degradation of HIF-1α [45]. The ubiquitination and degradation of HIF-1α was promoted by Parkin in breast cancer cells [46]. Under hypoxic conditions, HIF-1α is a major substrate of the VHL E3 ubiquitin ligase and instantly degraded through VHL-mediated ubiquitylation [47]. We observed reduced VHL expression and increased HIF-1α expression in the lungs of ARDS mice. As ARDS causes severe hypoxemia, it is possible that VHL targets HIF-1α for ubiquitylation and degradation in ARDS. In addition, we found that silencing of SPP1 enhanced VHL expression and reduced HIF-1α expression, suggesting that SPP1 might regulate VHL expression. Previous studies have demonstrated that SPP1 activates the STAT3 signaling [23], and STAT3 suppresses VHL-dependent degradation of HIF-1α by directly interacting with HIF-1α [48]. In this study, we demonstrated that SPP1 inhibited VHL expression and attenuated HIF-1α ubiquitination and degradation, thereby modulating the polarization of Th17, Treg, M1 and M2 in ARDS. Whether STAT3 is involved in this process in ARDS remains unclear and needs further investigation. Our data reveals a mechanism for HIF-1α degradation in ARDS and indicates that inhibition of SPP1 and upregulation of VHL in ARDS contribute to degrading HIF-1α, which may be targeted for ARDS treatment.

IL-10 and TGF-beta generally function as anti-inflammatory cytokines and Treg-derived IL-10 limits Th17 overshooting [49], but we did observe increased IL-10 and TGF-beta in blood and BALF samples. Actually, many studies have reported that IL-10 and TGF-beta are upregulated in ARDS animals and patients [50,51]. However, we do not know the mechanisms underlying the upregulation of IL-10 and TGF-beta in ARDS. One of our conjectures is that upregulation of anti-inflammatory cytokines such as IL-10 and TGF-beta is a compensatory mechanism to regulate the enhanced inflammation in ARDS, but it needs further exploration. Taken together, we firstly reported that increased expression of SPP1 exacerbated ARDS via disrupting the balance of Th17/Treg and M1/M2 through suppression of VHL expression and ubiquitination-dependent HIF-1α degradation. Although many trials of agents against inflammation have failed, inflammation remains a promising therapeutic target for ARDS. Our study not only deepens understanding of the pathogenesis of ARDS, but also provides promising biomarkers and therapeutic targets.

Ethics approval and consent to participate

Our experimental procedures were approved by the Ethics Committee of Chongqing General Hospital, and written informed consent was obtained from all patients.

Funding

Not applicable.

CRediT authorship contribution statement

Liang Chen: Conceptualization, Methodology, Visualization, Validation, Writing – original draft, Investigation, Supervision, Writing – review & editing. **Jin Yang:** Data curation. **Meng Zhang:** Software. **Donglin Fu:** Validation. **Huan Luo:** Methodology. **Xiaolei Yang:** Data curation.

Declaration of Competing Interest

The authors declare that they have no known competing financial interests or personal relationships that could have appeared to influence the work reported in this paper.

Data availability

Data will be made available on request.

Appendix A. Supplementary data

Supplementary data to this article can be found online at https://doi.org/10.1016/j.cyto.2022.156107.

References

[1] N.J. Meyer, L. Gattinoni, C.S. Calfee, Acute respiratory distress syndrome, Lancet 398 (10300) (2021) 622–637.
[2] A. Saguil, M.V. Fargo, Acute Respiratory Distress Syndrome: Diagnosis and Management, Am. Family Phys. 101 (12) (2020) 730–738.
[3] G.J. Bellingan, The pulmonary physician in critical care * 6: The pathogenesis of ALI/ARDS, Thorax 57 (6) (2002) 540–546.
[4] W.Y. Park, R.B. Goodman, K.P. Steinberg, J.T. Ruzinski, F. Radella 2nd, D.R. Park, J. Pugin, S.J. Skerrett, L.D. Hudson, T.R. Martin, Cytokine balance in the lungs of patients with acute respiratory distress syndrome, Am. J. Respirat. Crit. Care Med. 164 (10 Pt 1) (2001) 1896–1903.
[5] J.J.M. Wong, J.Y. Leong, J.H. Lee, S. Albani, J.G. Yeo, Insights into the immuno-pathogenesis of acute respiratory distress syndrome, Annals of translational medicine 7 (19) (2019) 504.
[6] P.L. Silva, P. Pelosi, P.R.M. Rocco, Personalized pharmacological therapy for ARDS: a light at the end of the tunnel, Expert Opin. Invest. Drugs 29 (1) (2020) 49–61.
[7] G. Lee, The Balance of Th17 versus Treg Cells in Autoimmunity, Int. J. Mol. Sci. 19 (3) (2018) 730.
[8] Z.X. Yu, M.S. Ji, J. Yan, Y. Cai, J. Liu, H.F. Yang, Y. Li, Z.C. Jin, J.X. Zheng, The ratio of Th17/Treg cells as a risk indicator in early acute respiratory distress syndrome, Crit. Care 19 (2015) 82.
[9] J. Chen, X. Zhang, J. Xie, M. Xue, L. Liu, Y. Yang, H. Qiu, Overexpression of TGFbeta1 in murine mesenchymal stem cells improves lung inflammation by impacting the Th17/Treg balance in LPS-induced ARDS mice, Stem Cell Res Ther 11 (1) (2020) 311.
[10] X. Chen, J. Tang, W. Shuai, J. Meng, J. Feng, Z. Han, Macrophage polarization and its role in the pathogenesis of acute lung injury/acute respiratory distress syndrome, Inflamm Res 69 (9) (2020) 883–895.
[11] G. Luan, F. Pan, L. Bu, K. Wu, A. Wang, X. Xu, Butorphanol Promotes Macrophage Phenotypic Transition to Inhibit Inflammatory Lung Injury via kappa Receptors, Front. Immunol. 12 (2021), 692286.
[12] S. Zhang, C. Chu, Z. Wu, F. Liu, J. Xie, Y. Yang, H. Qiu, IFIH1 Contributes to M1 Macrophage Polarization in ARDS, Front. Immunol. 11 (2020), 580838.
[13] S. Li, D. Qi, J.N. Li, X.Y. Deng, D.X. Wang, Vagus nerve stimulation enhances the cholinergic anti-inflammatory pathway to reduce lung injury in acute respiratory distress syndrome via STAT3, Cell Death Discovery 7 (1) (2021) 63.
[14] S. Chen, N. Sang, Hypoxia-Inducible Factor-1: A Critical Player in the Survival Strategy of Stressed Cells, J. Cell. Biochem. 117 (2) (2016) 267–278.
[15] E.V. Dang, J. Barbi, H.Y. Yang, D. Jinasena, H. Yu, Y. Zheng, Z. Bordman, J. Fu, Y. Kim, H.R. Yen, W. Luo, K. Zeller, L. Shimoda, S.L. Topalian, G.L. Semenza, C. V. Dang, D.M. Pardoll, F. Pan, Control of T(H)17/T(reg) balance by hypoxia-inducible factor 1, Cell 146 (5) (2011) 772–784.
[16] T. Wang, H. Liu, G. Lian, S.Y. Zhang, X. Wang, C. Jiang, HIF1alpha-Induced Glycolysis Metabolism Is Essential to the Activation of Inflammatory Macrophages, Mediators Inflamm. 2017 (2017) 9029327.
[17] B. Zhong, J. Du, F. Liu, Y. Liu, S. Liu, L. Xie, D. Wang, L. Ba, Activation of the mTOR/HIF-1alpha/VEGF axis promotes M1 macrophage polarization in non-eosCRSwNP, Allergy (2021).
[18] M. Xu, F.L. Cao, Y.F. Zhang, L. Shan, X.L. Jiang, X.J. An, W. Xu, X.Z. Liu, X. Y. Wang, Tanshinone IIA therapeutically reduces LPS-induced acute lung injury by inhibiting inflammation and apoptosis in mice, Acta Pharmacol. Sin. 36 (2) (2015) 179–187.
[19] S. Palanidurai, J. Phua, Y.H. Chan, A. Mukhopadhyay, P/FP ratio: incorporation of PEEP into the PaO2/FiO2 ratio for prognostication and classification of acute respiratory distress syndrome, Ann. Intensive Care 11 (1) (2021) 124.
[20] L. Van Hoecke, E.R. Job, X. Saelens, K. Roose, Bronchoalveolar Lavage of Murine Lungs to Analyze Inflammatory Cell Infiltration, Journal of visualized experiments : JoVE 123 (2017).
[21] M. Bhatia, S. Moochhala, Role of inflammatory mediators in the pathophysiology of acute respiratory distress syndrome, J. Pathol. 202 (2) (2004) 145–156.
[22] C. Song, H. Li, Y. Li, M. Dai, L. Zhang, S. Liu, H. Tan, P. Deng, J. Liu, Z. Mao, Q. Li, X. Su, Y. Long, F. Lin, Y. Zeng, Y. Fan, B. Luo, C. Hu, P. Pan, NETs promote ALI/ARDS inflammation by regulating alveolar macrophage polarization, Exp. Cell Res. 382 (2) (2019), 111486.
[23] R. Behera, V. Kumar, K. Lohite, S. Karnik, G.C. Kundu, Activation of JAK2/STAT3 signaling by osteopontin promotes tumor growth in human breast cancer cells, Carcinogenesis 31 (2) (2010) 192–200.
[24] C. Zhang, K. Ma, W.Y. Li, IL-6 Promotes Cancer Stemness and Oncogenicity in U2OS and MG-63 Osteosarcoma Cells by Upregulating the OPN-STAT3 Pathway, J. Cancer 10 (26) (2019) 6511–6525.
[25] A.F. McGettrick, L.A.J. O'Neill, The Role of HIF in Immunity and Inflammation, Cell Metab. 32 (4) (2020) 524–536.
[26] S.V. Baudouin, Manipulation of inflammation in ARDS: achievable goal or distant target? Thorax 61 (6) (2006) 464–465.
[27] N. Clemente, D. Raineri, G. Cappellano, E. Boggio, F. Favero, M.F. Soluri, C. Dianzani, C. Comi, U. Dianzani, A. Chiocchetti, Osteopontin Bridging Innate and Adaptive Immunity in Autoimmune Diseases, J. Immunol. Res. 2016 (2016) 7675437.
[28] S. Caputo, M. Bellone, Osteopontin and the immune system: another brick in the wall, Cell. Mol. Immunol. 15 (4) (2018) 405–407.
[29] G. Murugaiyan, A. Mittal, H.L. Weiner, Increased osteopontin expression in dendritic cells amplifies IL-17 production by CD4+ T cells in experimental autoimmune encephalomyelitis and in multiple sclerosis, J. Immunol. 181 (11) (2008) 7480–7488.
[30] S. Sangaletti, C. Tripodo, S. Sandri, I. Torselli, C. Vitali, C. Ratti, L. Botti, A. Burocchi, R. Porcasi, A. Tomirotti, M.P. Colombo, C. Chiodoni, Osteopontin shapes immunosuppression in the metastatic niche, Cancer Res. 74 (17) (2014) 4706–4719.
[31] T. Alissafi, E. Kourepini, D.C.M. Simoes, N. Paschalidis, M. Aggelakopoulou, T. Sparwasser, L. Boon, H. Hammad, B.N. Lambrecht, V. Panoutsakopoulou, Osteopontin Promotes Protective Antigenic Tolerance against Experimental Allergic Airway Disease, J. Immunol. 200 (4) (2018) 1270–1282.
[32] K. Schuch, B. Wanko, K. Ambroz, A. Castelo-Rosa, V. Moreno-Viedma, N.G. Grun, L. Leitner, G. Staffler, M. Zeyda, T.M. Stulnig, Osteopontin affects macrophage polarization promoting endocytic but not inflammatory properties, Obesity 24 (7) (2016) 1489–1498.
[33] F. Takahashi, K. Takahashi, K. Shimizu, R. Cui, N. Tada, H. Takahashi, S. Soma, M. Yoshioka, Y. Fukuchi, Osteopontin is strongly expressed by alveolar macrophages in the lungs of acute respiratory distress syndrome, Lung 182 (3) (2004) 173–185.
[34] K. Nakai, Multiple roles of macrophage in skin, J. Dermatol. Sci. 104 (1) (2021) 2–10.
[35] D.M. Mosser, J.P. Edwards, Exploring the full spectrum of macrophage activation, Nat. Rev. Immunol. 8 (12) (2008) 958–969.
[36] Y. Yao, X.H. Xu, L. Jin, Macrophage Polarization in Physiological and Pathological Pregnancy, Front. Immunol. 10 (2019) 792.
[37] G.W. Tu, Y. Shi, Y.J. Zheng, M.J. Ju, H.Y. He, G.G. Ma, G.W. Hao, Z. Luo, Glucocorticoid attenuates acute lung injury through induction of type 2 macrophage, J. Transl. Med. 15 (1) (2017) 181.
[38] M.V. Suresh, S. Balijepalli, B. Zhang, V.V. Singh, S. Swamy, S. Panicker, V. A. Dolgachev, C. Subramanian, S.K. Ramakrishnan, B. Thomas, T.C. Rao, M. J. Delano, D. Machado-Aranda, Y.M. Shah, K. Raghavendran, Hypoxia-Inducible Factor (HIF)-1alpha Promotes Inflammation and Injury Following Aspiration-Induced Lung Injury in Mice, Shock 52 (6) (2019) 612–621.
[39] E.T. Clambey, E.N. McNamee, J.A. Westrich, L.E. Glover, E.L. Campbell, P. Jedlicka, E.F. de Zoeten, J.C. Cambier, K.R. Stenmark, S.P. Colgan, H. K. Eltzschig, Hypoxia-inducible factor-1 alpha-dependent induction of FoxP3 drives regulatory T-cell abundance and function during inflammatory hypoxia of the mucosa, Proceedings of the National Academy of Sciences of the United States of America 109 (41) (2012) E2784–E2793.
[40] J. Ben-Shoshan, S. Maysel-Auslender, A. Mor, G. Keren, J. George, Hypoxia controls CD4+CD25+ regulatory T-cell homeostasis via hypoxia-inducible factor-1alpha, Eur. J. Immunol. 38 (9) (2008) 2412–2418.
[41] H. Jiang, Y. Huang, H. Xu, R. Hu, Q.F. Li, Inhibition of hypoxia inducible factor-1alpha ameliorates lung injury induced by trauma and hemorrhagic shock in rats, Acta Pharmacol. Sin. 33 (5) (2012) 635–643.
[42] M.V. Suresh, S.K. Ramakrishnan, B. Thomas, D. Machado-Aranda, Y. Bi, N. Talarico, E. Anderson, S.M. Yatrik, K. Raghavendran, Activation of hypoxia-inducible factor-1alpha in type 2 alveolar epithelial cell is a major driver of acute inflammation following lung contusion, Critical care medicine 42 (10) (2014) e642–e653.
[43] T. Eckle, K. Brodsky, M. Bonney, T. Packard, J. Han, C.H. Borchers, T.J. Mariani, D. J. Kominsky, M. Mittelbronn, H.K. Eltzschig, HIF1A reduces acute lung injury by optimizing carbohydrate metabolism in the alveolar epithelium, PLoS biology 11 (9) (2013), e1001665.
[44] M.J. Clague, S. Urbe, Ubiquitin: same molecule, different degradation pathways, Cell 143 (5) (2010) 682–685.
[45] M.Y. Koh, B.G. Darnay, G. Powis, Hypoxia-associated factor, a novel E3-ubiquitin ligase, binds and ubiquitinates hypoxia-inducible factor 1alpha, leading to its oxygen-independent degradation, Mol. Cell. Biol. 28 (23) (2008) 7081–7095.
[46] J. Liu, C. Zhang, Y. Zhao, X. Yue, H. Wu, S. Huang, J. Chen, K. Tomsky, H. Xie, C. A. Khella, M.L. Gatza, D. Xia, J. Gao, E. White, B.G. Haffty, W. Hu, Z. Feng, Parkin targets HIF-1alpha for ubiquitination and degradation to inhibit breast tumor progression, Nat. Commun. 8 (1) (2017) 1823.
[47] S. Paltoglou, B.J. Roberts, HIF-1alpha and EPAS ubiquitination mediated by the VHL tumour suppressor involves flexibility in the ubiquitination mechanism, similar to other RING E3 ligases, Oncogene 26 (4) (2007) 604–609.
[48] J.E. Jung, H.S. Kim, C.S. Lee, Y.J. Shin, Y.N. Kim, G.H. Kang, T.Y. Kim, Y.S. Juhnn, S.J. Kim, J.W. Park, S.K. Ye, M.H. Chung, STAT3 inhibits the degradation of HIF-1alpha by pVHL-mediated ubiquitination, Exp. Mol. Med. 40 (5) (2008) 479–485.
[49] C.A. Stewart, H. Metheny, N. Iida, L. Smith, M. Hanson, F. Steinhagen, R. M. Leighty, A. Roers, C.L. Karp, W. Muller, G. Trinchieri, Interferon-dependent IL-10 production by Tregs limits tumor Th17 inflammation, J. Clin. Invest. 123 (11) (2013) 4859–4874.
[50] R.J. Fahy, F. Lichtenberger, C.B. McKeegan, G.J. Nuovo, C.B. Marsh, M.D. Wewers, The acute respiratory distress syndrome: a role for transforming growth factor-beta 1, Am. J. Respir. Cell Mol. Biol. 28 (4) (2003) 499–503.
[51] J. Wang, X. Yang, Y. Li, J.A. Huang, J. Jiang, N. Su, Specific cytokines in the inflammatory cytokine storm of patients with COVID-19-associated acute respiratory distress syndrome and extrapulmonary multiple-organ dysfunction, Virol. J. 18 (1) (2021) 117.